Anal. Methods Environ. Chem. J. 7 (4) (2024) 17-32

AMECJ

Research Article, Issue 4
Analytical Methods in Environmental Chemistry Journal
Journal home page: www.amecj.com/ir

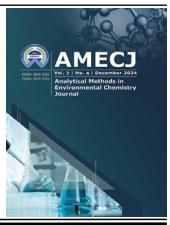

Evaluation and quantification of Fe_3O_4 concentrations in deposits formed inside Iraqi gas supply pipelines using a chemiluminescence method based on flow injection analysis

Nagham S. Al-Awadi[a], Zaineb Falah Hassan[b] and Hussein Fares Abd-Alrazack[c*]
[a] *Department of Chemistry College of Science, University of Baghdad, Baghdad, Iraq*
[b] *Petroleum research & development center, Iraq*
[c] *National Oil Company, Iraq Drilling Company, Baghdad, Iraq*

ARTICLE INFO:
Received 6 Aug 2024
Revised form 27 Oct 2024
Accepted 18 Nov 2024
Available online 30 Dec 2024

Keywords:
Chemiluminescence,
Flow injection analysis,
Gas pipelines contamination,
Iron oxide,
Black powder

ABSTRACT
The accumulation of black powder deposits inside gas pipelines can lead to various issues affecting pipeline operation and integrity. The presence of black powder has the potential to contaminate the gas product, promote increased wear on pipeline internals, and cause clogging that reduces flow rates. From a safety perspective, black powder buildup may pose health and environmental concerns. Previous studies have analyzed the composition of black powder deposits from pipelines using techniques like XRF, XRD, TG-DTA, and FTIR. Their findings show that Iron oxide (Fe_3O_4) is the primary component of black powder. This study developed a novel flow injection-chemiluminescence (FI-CL) method under basic conditions for determining Fe_3O_4 concentrations in black powder deposits because Fe_3O_4 can catalyze the chemiluminescence reaction. Compared to traditional analytical techniques, the proposed CL-based flow injection approach is characterized by good selectivity, simplicity, low cost, and without consuming additional materials. The CL mechanism was investigated through CL spectral, revealing the involvement of Fe_3O_4 in enhancing the luminol-NaOH-H_2O_2 reaction. Experimental conditions for the FI-CL system were optimized. Under optimal parameters, the relative CL intensity showed a linear relationship with Fe_3O_4 concentration over the range of 0.5-100 µg mL^{-1}, and the detection limit was 0.47 µg mL^{-1} with a relative standard deviation (%RSD) of 2.0% at 5.0 µg mL^{-1}. The method was successfully applied to black powder samples extracted from gas pipelines, showing 92.59-107.69% recoveries and a precision of 0.8-3.1%. Results agreed well with an alternative technique. The proposed FI-CL method offers a fast, convenient, and cost-effective means for iron oxide quantification in pipeline deposits and corrosion products.

1. Introduction

Natural gas has gained widespread use as a relatively clean energy source for industrial and domestic applications. Continuous supply and delivery of natural gas relies on extensive pipeline transmission networks that transport the fuel over long distances. As demand for natural gas grows, ongoing development and expansion of these pipeline infrastructures are necessary [1, 2]. However, pipelines present unique engineering challenges due to their large scales, diverse terrains

*Corresponding Author: Hussein Fares Abd-Alrazack
Email: hiban2127@gmail.com
https://doi.org/10.24200/amecj.v7.i04.332

traversed, and exposure to high operating pressures and temperatures during gas transmission. Pipeline materials and diameters must be carefully selected to ensure structural integrity under the demanding operating conditions experienced over decades of service. Reliable transportation of natural gas hinges on pipelines maintaining pressure containment across various geographies and weather patterns throughout their lifespan [3, 4]. The formation of black powder deposits on the internal pipeline surfaces can impact the underground transportation of natural gas through pipelines. Black powder accumulates due to corrosion processes occurring when trace amounts of water and oxygen interact with the gas and pipe material composition. Black powder poses several disadvantages to natural gas quality and efficient transport [5-9]. Black powder deposits can contaminate the gas stream and potentially compromise gas specifications. Its buildup also increases drag forces on the flowing gas, restricting flow rates and resulting in lost pipeline capacity. From a material integrity standpoint, black powder exacerbates pipeline corrosion and erosion problems [10, 11]. Its abrasive nature accelerates pipeline wear and weakens the pipe wall. Additionally, loose black powder particles risk plugging instrumentation lines and valves if mobilized [12]. Previous characterization studies have shown that black powder predominantly comprises iron oxide compounds such as magnetite (Fe_3O_4) and ferric sulfides [13]. As a product of corrosion reactions involving iron-based steel pipelines, iron oxides are the primary constituent species within black powder. Corrosion of steel pipelines under typical operating conditions leads to the formation of iron oxides. The main corrosion products of iron gas pipelines contain iron (II, III) oxide compounds. Recent reports suggest several possible origins for the iron oxides observed in deposit buildup. One potential source is milling scale, a persistent iron (II, III) oxide that adheres to pipe surfaces during high-temperature manufacturing. Another is flash rust containing Fe_2O_3 and FeO_2H from hydro-testing water exposure. Ongoing internal corrosion within operating pipelines can contribute to black powder iron oxide content [12, 14-16]. Accurate quantification of iron oxide levels in deposited black powder can provide insight into pipeline corrosion behavior and predict future challenges from deposit formation. However, traditional analytical techniques for iron oxide determination, such as microwave [17], thermal analysis [18], Ion mobility-mass spectrometry [19], X-ray Fluorescence [20], Infrared desorption [21], Solid-Liquid gas phase extraction [22, 23], colorimetry [24, 25], flow injection [26-28] and X-ray [29], are often complicated, time-consuming and costly. Chemiluminescence (CL) techniques have gained significant interest in analytical applications due to their inherent advantages over other methods. Compared to traditional approaches, CL assays often have lower detection limits, higher sensitivity, more comprehensive linear dynamic ranges, shorter analysis times, and more straightforward instrumentation requirements. These attributes have supported the extensive use of CL in diverse areas of analytical chemistry, such as environmental monitoring, biomedical analysis, and materials characterization [30-34]. Determination of analytes by CL avoids many of the limitations of other approaches. Iron oxide is a primary constituent of black powder deposits formed through corrosion processes in natural gas pipelines. Determining iron oxide concentrations within these deposits provides insight into the extent and causes of internal corrosion over time. Higher iron oxide levels may indicate increased wall thinning and weakening of the pipe material. This influences integrity assessment and replacement scheduling. Additionally, iron oxides can catalyze exothermic reactions when exposed to hydrogen under certain conditions. Quantifying iron oxide concentrations helps assess the propensity for self-heating and potentially dangerous temperature escalations within pockets of built-up deposits. While various analytical techniques exist, there remains a need for sensitive, selective, and convenient methods. Chemiluminescence-based assays address these needs but require a suitable catalyst system. Recent

studies have shown that iron oxide nanoparticles can strongly catalyze the chemiluminescence reaction between luminol and hydrogen peroxide [35, 36]. Iron oxides are highly effective catalysts that accelerate the reaction kinetics and enhance light output. The mechanism is believed to involve the Fenton-like redox cycling of Fe ions to generate reactive oxygen species, resulting in intensified oxidation of luminol. Significantly, the chemiluminescence intensity produced has been demonstrated to correlate directly with iron oxide concentration over a wide range. Therefore, a facile method for sensitive and selective iron oxide determination can be developed by leveraging the catalytic properties of iron oxides to boost chemiluminescence to quantifiable levels. However, to our knowledge, CL-based determination of iron oxide concentrations under basic conditions has not been reported.

This work aims to develop a novel chemiluminescence-based technique for determining iron oxide concentrations in black powder formed within natural gas pipelines. The study will optimize a flow injection chemiluminescence (CL-FI) method leveraging the enhancing effect of iron oxides on the luminol-NaOH-H_2O_2 system. Pairing such compositional data obtained through efficient analytical techniques (CL-FI) with a systematic compilation of historical operational parameters and pipeline design/material selection records would allow for developing kinetic models linking deposition rates to influencing factors. Such predictive models, incorporating cross-sectional concentration profiling and longitudinal operational data, can potentially optimize pipeline maintenance planning.

2. Experimental

2.1. Materials

All chemicals used were of at least analytical reagent grade. Ultrapure deionized water was used for all solution preparations and dilutions. A 100 µg mL^{-1} stock solution of luminol (3-aminophthal-hydrazide, CAS No:521-31-3, Sigma-Aldrich) was prepared by dissolving 1.0 mg in 100 mL of 0.05 mmol L^{-1} sodium carbonate (CAS No:497-19-8, Sigma-Aldrich) solution. A 100-µg mL^{-1} hydrogen peroxide (H_2O_2, 30% v/v, CAS No: 87003-224, BDH) working solution was obtained by diluting 5.15 mL of the commercial solution to 500 mL with ultrapure water. The standardized solution was verified against a potassium permanganate standard (CAS No:7722-64-7, Sigma-Aldrich). To prepare 100 mL of a 1000 mg L^{-1} of Fe_3O_4 standard solution (CAS No: 1317-61-9, Sigma-Aldrich), 0.01 g of iron (II, III) oxide powder (Fe_3O_4) is accurately weighed using an analytical balance. The Fe_3O_4 is transferred to a clean, dry 100 mL beaker. 10 mL of concentrated hydrochloric acid (HCl, CAS No: 7647-01-0, BDH) is then added to the beaker to dissolve the iron oxide. The beaker is placed on a magnetic stir plate, and the solution is stirred for 30 minutes to ensure complete dissolution of the Fe_3O_4. Once dissolution is confirmed, the beaker's contents are quantitatively transferred to a 100 mL volumetric flask using deionized water to rinse any residue off the walls. The volumetric flask is then filled to the 100 mL graduation line with deionized water. The solution is mixed thoroughly by inverting the flask several times. All stock and working solutions were stored in amber bottles at 4ºC when not in use. Fresh preparations were made as needed to maintain reagent integrity throughout experiments.

2.2. Apparatus

The FI-CL system configuration is shown in Figure 1. Reagent and sample delivery was facilitated by multi-channel peristaltic pumps (HL-2D, Shanghai BQ Instruments). Polytetrafluoroethylene (PTFE) tubing (0.8 mm internal diameter) was employed to interconnect all components. A six-port injection valve (Rheodyne, USA) equipped with a 100 µL sample loop was used to introduce samples into the flowing carrier stream. Chemiluminescence signals were measured using an ultraweak luminescence analyzer (Institute of Biophysics, Beijing, China). This detector utilizes a flat spiral flow cell interfaced with a photomultiplier tube (RCA 931A, UK). Data

acquisition and processing were performed using the accompanying software. The photomultiplier tube was powered by a stable high-voltage power supply (Jobin Yvon, France) operated over the 0-1.6 kV range. Signals from the photomultiplier were amplified using a low-noise preamplifier (United Detector Technology, USA) before interfacing with a data recording instrument. A Kompen Sograph Model C1032 recorder (Siemens, Germany) was used to measure the amplified chemiluminescence signals over 1-500 mV as a linear range. This provided analog tracing of the light emission dynamics throughout kinetic experiments.

2.3. General Procedure

The FI-CL method was straightforward to implement. As illustrated in Figure 1, the peristaltic pumps continuously propelled the luminol, H_2O_2, double distilled water (carrier stream), NaOH, and sample solutions (either a standard or unknown sample containing the analyte) through the system at 2.0 mL min^{-1} of flow rate. Initially, the general procedure involved three main steps. At the first confluence point Y_1, a 0.5 mmol L^{-1} sodium hydroxide solution was combined and mixed with the luminol solution 0.5 mmol L^{-1} to form the dianion luminol. Secondly, a hydrogen peroxide solution of 0.006 mmol L^{-1} was pumped via a peristaltic pump and merged with the dianion luminol stream at the secondary confluence point Y_2. Finally, when the injection valve was switched to injection mode, the carrier flow delivered the standard or sample solution downstream to the tertiary confluence point Y_3. At Y_3, the standard/sample merged with the mixed hydrogen peroxide and dianion luminol stream. This allowed for online chemiluminescence detection from the resultant reaction as the combined stream passed through the flow cell for measurement. With the injection valve in the load position initially, the H_2O_2 solution merged with the luminol-NaOH mixture at the second confluence point (Y_2). It flowed through the entire flow system to establish a stable baseline signal. Once baseline stabilization was achieved, the injection valve was switched to the inject position. This allowed the distilled water carrier to transport the contents of the 100 µL sample loop directly into the flowing reaction stream within the flow cell. The ensuing chemiluminescent emission was simultaneously measured and recorded. Mixing coils (M_1-M_3) were included at various points throughout the flow lines to facilitate the complete intermixing of the components in the moving fluid stream.

2.4. Sample preparation of black powder

Black powder deposit samples were collected from the inner surfaces of in-service natural gas transmission pipelines near Karbala, Mosul, and Diwaniya, Iraq. These three sites were selected to represent different

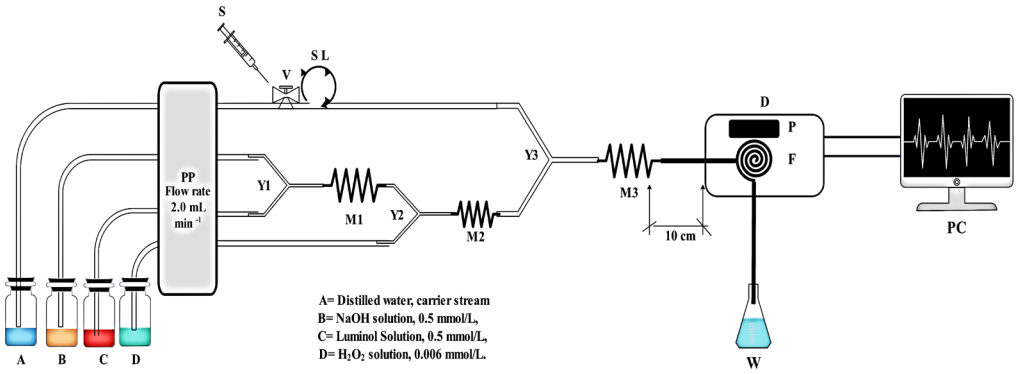

Fig. 1. Schematic diagram of the chemiluminescence-flow injection (CL-FI) system configuration for determining Fe_3O_4. A: carrier stream (MQ water); B: NaOH 0.5 mmol L^{-1}; C: luminol solution 0.5 mmol L^{-1}, H_2O_2 0.006 mmol L^{-1}, PP: peristaltic pump; S: syringe for injection of standard or sample; V: six ports injection valve; SL: sample loop; Y_1-Y_3: confluence points; M_1-M_3: 30 cm mixing coils; D: chemiluminescence detector; P: photomultiplier tube; F: flow cell; w: waste; PC: personal computer.

geographic regions across the country as the pipelines transport gas from fields to power plants in Karbala, Mosul, and Diwaniya provinces. Pipe spool pieces approximately 15 km upstream from the major gas delivery stations were extracted for sampling. Pipelines selected represented a range of diameters (6-24 inches) and compositions (carbon steel). Samples were scraped directly from the pipe wall using a cleaned stainless-steel spatula and placed into pre-cleaned polyethylene containers. The pretreatment step to selectively isolate Fe_3O_4 is important before further analysis of black powder samples collected from pipe walls. A 0.5 g subsample was weighed out and pretreated following the method of Chen and his colleagues [41]. First, the subsample was added to a beaker containing 6M HCl and refluxed for 1 hour with occasional stirring, which dissolved any carbonates and sulfides in the sample. Then, 30% H_2O_2 was slowly added, and heating continued for an additional hour to oxidize any Fe^{2+} to the Fe^{3+} state. The pretreated residue was vacuum filtrated through a Whatman #41 filter paper. The residue on the filter paper was washed with deionized water until the filtrate reached neutral pH. Subsequently, the pretreated residue was dried overnight at 80°C and weighed to calculate recovery. Next, the dried pretreated residue was resuspended in deionized water and separated magnetically using a neodymium magnet. The Fe_3O_4 fraction was attracted to the side of the vial nearest the magnet and decanted, while the supernatant containing non-magnetic fractions was discarded. Finally, the Fe_3O_4 fraction was washed 3 times with deionized water. This procedure selectively isolates Fe_3O_4 from the black powder sample before further digestion and analysis, removing potential interference from Fe^{2+} ions. To prepare the sample for the FL-CL reaction, the samples were air-dried for 24 hours in the laboratory, then gently ground with an agate mortar and pestle to homogenize and break up agglomerates. The powdered solids were then sieved through a 150 µm mesh to obtain a fine fraction suitable for acid digestion. The sieved black powder was accurately transferred into digestion vessels. A mixture of 25 mL concentrated HNO_3 and 10 mL concentrated HCl was added to each vessel, and the solutions were heated to 95ºC for 2 hours with reflux to digest the solid phase fully. After cooling, the extracts were filtered through Whatman No. 42 filter paper into 100 mL volumetric flasks and made up to the mark with 2% HNO_3 [42]. These prepared sample solutions were analyzed using the proposed method (CL-FI) to quantify levels of iron oxide content in the original black powder deposits.

3. Results and Discussion

The literature reports black powder forms due to dissolved oxygen corrosion caused by small amounts of oxygen and water in the gas stream reacting with pipe material. Quantifying the concentration of Fe_3O_4 present in black powder deposits at different time points during pipeline operation can provide valuable insight into the rate and dynamics of corrosion product accumulation over time. The method proposed in this study is more sensitive, speedy, and simple than numerous other reported analytical methods (Table 1).

Table 1. The proposed CL-FI for the determination of iron oxide exhibits excellent linearity compared to other analytical techniques.

Used Methods	LR (µg mL^{-1})	Remarks	References
FAAS	0.2-90	More sensitive but narrow response range	[37]
HPLC/MS	0.05–20	More sensitive but low response range	[38]
Colorimetric	12.0-120.9	Less sensitive	[39]
Electrochemical	2.0-60	Less sensitive	[40]
CL-FI	0.5-100	Using a simple instrument and more sensitive	This work

LR: Linearity Range
Note: The sensitivity of the analytical method is represented by the lowest concentration in the calibration curve that can be accurately and precisely quantified

3.1. Kinetic study

Before developing the FI-CL method, the kinetic characteristics of the proposed chemiluminescent reaction between luminol, H_2O_2, NaOH, and Fe_3O_4 were investigated using a batch approach. In the batch setup, experimental conditions were held constant while the intensity-time profile of the luminol-NaOH-H_2O_2- Fe_3O_4 system was recorded to study the reaction kinetics. As shown in Figure 2, the CL system exhibited a rapid response. The CL intensity peak appeared within 0.5 seconds of luminol-NaOH-H_2O_2 solution injection and quickly decreased to the baseline level within 10 seconds. These results demonstrated that Fe_3O_4 effectively enhances the weak luminescence of the luminol-NaOH-H_2O_2 system. Therefore, the CL method provides a fast and sensitive means for Fe_3O_4 determination. The brief kinetic window is suitable for flowing injection analysis, where samples are rapidly introduced and swept through the flow cell.

3.2. The effect of luminol solution

The CL reaction between Fe_3O_4, luminol, NaOH, and H_2O_2 involves the oxidation of luminol by the reaction of H_2O_2 with the iron oxide (oxidizing agent). The concentration of luminol impacts both the assay sensitivity and linear dynamic range. The effect of luminol concentration on the resulting CL intensity was evaluated in the 0.05-1.0 mmol range. L^{-1}. As shown in Figure 3, the CL signal increased with rising luminol concentration up to 0.5 mmol. L^{-1}. Above this level, a decrease in CL intensity was observed, likely due to self-absorption of the higher concentration of brightly colored product. A luminol concentration of 0.5 mmol. L^{-1} provided the maximum signal response. Therefore, this optimal concentration was carried forward for subsequent optimization studies and analytical method development.

3.3. Effect of H_2O_2 concentration

H_2O_2 is the oxidizing agent in the CL reaction between luminol, NaOH, and the analyte. Its concentration, therefore, significantly impacts the resulting CL signal intensity. To determine the optimal H_2O_2 concentration, its effect was studied over the range of 0.002-0.07 mmol L^{-1}, keeping all other reaction conditions constant. As shown in Figure 4, the CL intensity increased with rising H_2O_2 concentration up to 0.006 mmol L^{-1}. Beyond this level, further increases in peroxide concentration resulted in decreased

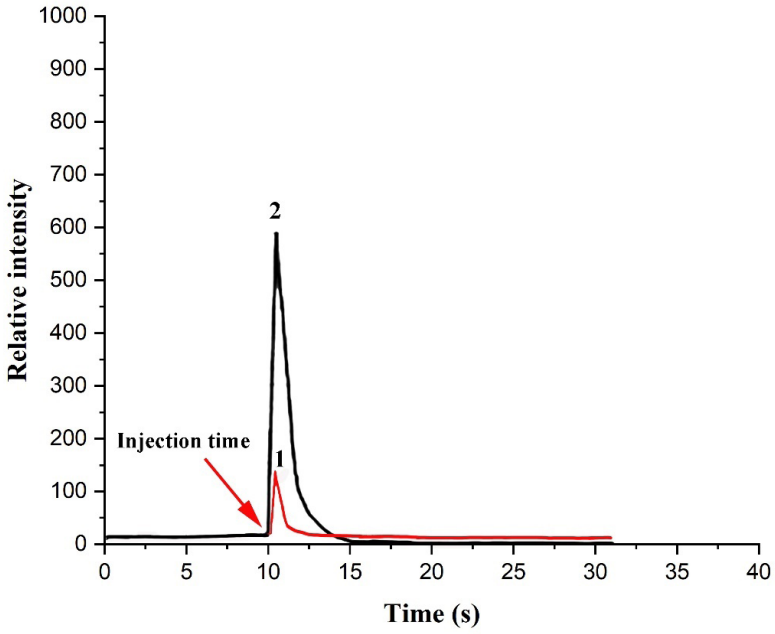

Fig. 2. Kinetic curves of luminol-H_2O_2-NaOH system. (1) Using of mixture of luminol-H_2O_2-NaOH and water system without Fe_3O_4; (2) 100 µL Fe_3O_4 injected into the mixture of luminol-H_2O_2-NaOH system. Luminol: 0.4 mmol/L; H_2O_2: $2x10^{-3}$ mmol L^{-1}; NaOH: 0.5 mmol L^{-1}; Fe_3O_4: 50 µg mL^{-1}

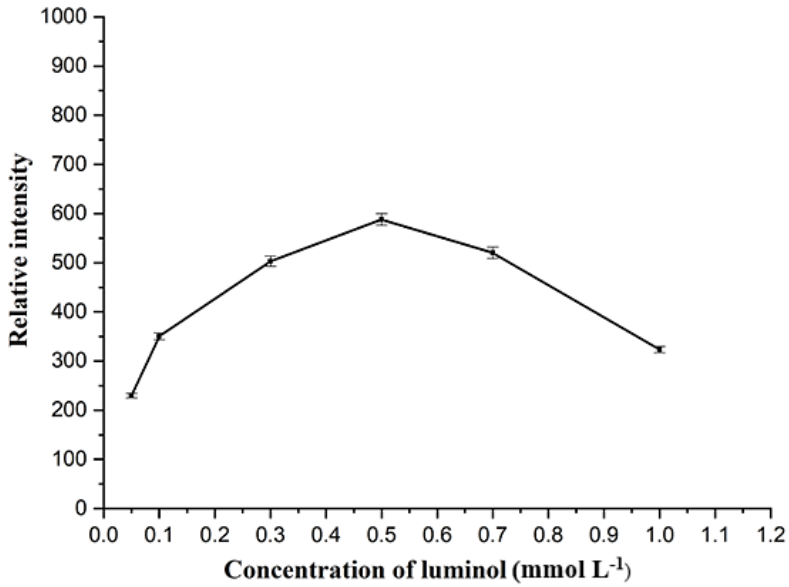

Fig. 3. Effect of luminol concentration on the CL intensity for the determination of Fe_3O_4using the proposed CL-FI method under the following experimental conditions: Flow rate 2.0 mL min^{-1}; sample loop 100 µL; NaOH concentration 0.3 mmol L^{-1}; H_2O_2 concentration 0.004 mmol L^{-1}; Fe_3O_4: 50 µg mL^{-1}

light output. The mechanism of the CL process can explain this observation. At lower H_2O_2 levels, the availability of oxidizing agents limits the reaction kinetics. However, increasing the concentration of H_2O_2 above 0.006 mmol L^{-1} did not lead to any additional enhancement of the CL intensity. The maximum CL intensity obtained at 0.006 mmol L^{-1} H_2O_2 indicates this concentration provides the ideal balance between sufficient oxidation power and avoidance of catalytic interference. Therefore, 0.006 mmol L^{-1} was selected as the optimum H_2O_2 concentration and used in subsequent method optimization and analytical applications to ensure maximum assay sensitivity and performance.

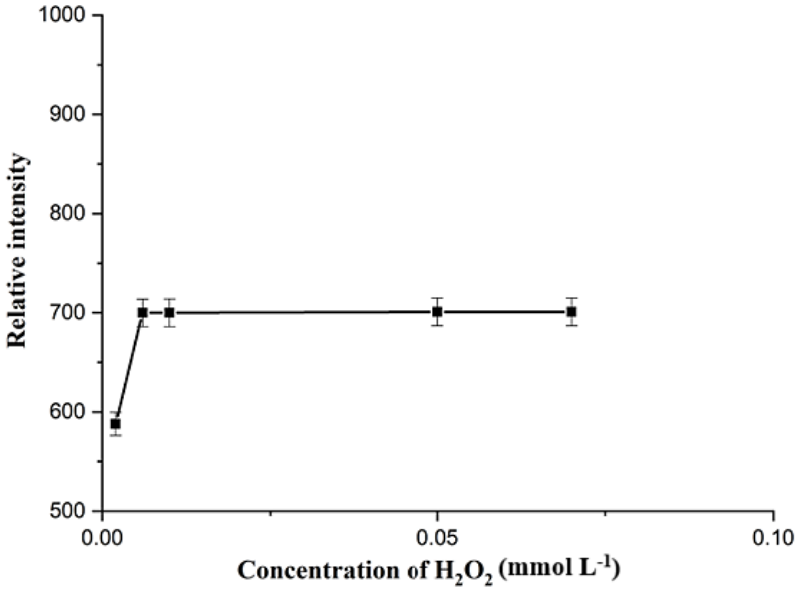

Fig. 4. Effect of H_2O_2 concentration on the CL intensity for the determination of Fe_3O_4 using the proposed CL-FI method under the following experimental conditions: Flow rate 2.0 mL min^{-1}; sample loop 100 µL; NaOH concentration 0.3 mmol L^{-1}; luminol concentration 0.5 mmol L^{-1}; Fe_3O_4: 50 µg mL^{-1}

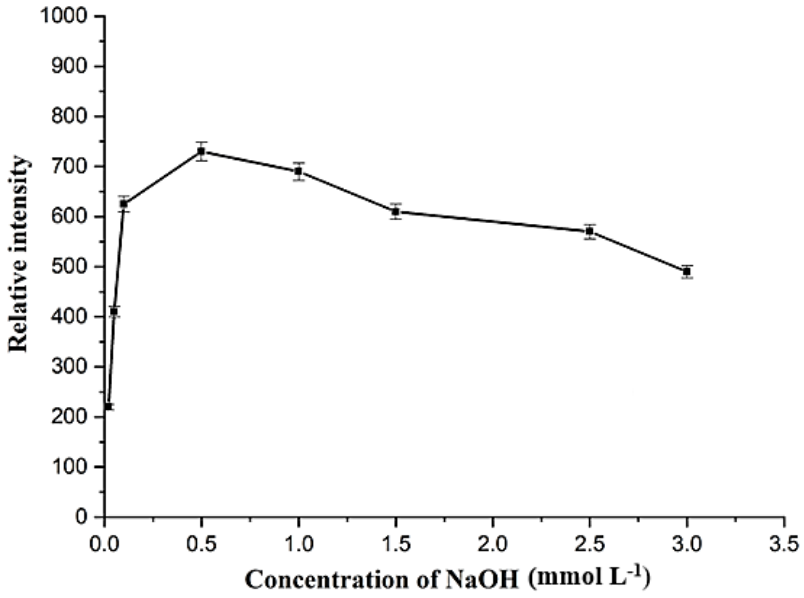

Fig. 5. Effect of NaOH concentration on the CL intensity for the determination of Fe_3O_4 using the proposed CL-FI method under the following experimental conditions: Flow rate 2.0 mL min^{-1}; sample loop 100 µL; H_2O_2 concentration 0.006 mmol L^{-1}; luminol concentration 0.5 mmol L^{-1}; Fe_3O_4: 50 µg mL^{-1}

3.4. The effect of basic medium

NaOH enhances the chemiluminescent reaction between luminol and the oxidizing agent. The effect of NaOH concentration, ranging from 0.02 mol L^{-1} to 2.0 mol L^{-1}, was examined. As shown in Figure 5, the CL intensity of the luminol-H_2O_2-Fe_3O_4 system increased with rising NaOH concentration up to 0.5 mol L^{-1}. Beyond this level, further increases in base concentration led to decreased light output. The reaction mechanism can explain this observation. At lower concentrations, the basic environment is insufficient to deprotonate reagents and initiate the chemiluminescent oxidative cleavage of luminol. However, above 0.5 mol L^{-1} NaOH, the excess hydroxyl ions may interfere with the reaction kinetics rather than catalyze it. Therefore, 0.5 mol L^{-1} NaOH optimized the balance between developing an alkaline environment conducive to redox signaling without introducing interfering effects. This concentration of sodium hydroxide solution was carried forward for subsequent experimentation.

3.5. Optimization of FI-CL conditions

Several flow parameters were optimized to achieve maximum CL output while maintaining efficient analyte processing. Using 30 cm reaction coils, flow rates from 0.4 to 4.0 mL min^{-1} were evaluated for their effects on signal intensity and peak characteristics. Lower flow rates enhanced chemiluminescence as they allowed longer contact time between reagents. However, extremely slow flows produced overly broad peaks and lengthy analysis times; meanwhile, higher flow rates reduced signal by shortening the reaction window. The optimal balance was 2.0 mL min^{-1}, as this flow rate provided sufficient time for the chemiluminescent reaction while avoiding peak widening or throughput limitations. Injection loop volumes from 25-200 µL were also examined. Larger loops generated broader peaks undesirable for sensitivity, while smaller volumes diminished the signal. A 100 µL injection volume demonstrated the best signal-to-noise ratio. These flow optimization studies enabled the maximization of analytical parameters for accurate and precise analyte quantitation using this flow injection chemiluminescence system, as shown in Figures 6 and 7. Also, Table 2 summarizes the optimized experimental conditions for the flow injection chemiluminescence methodology.

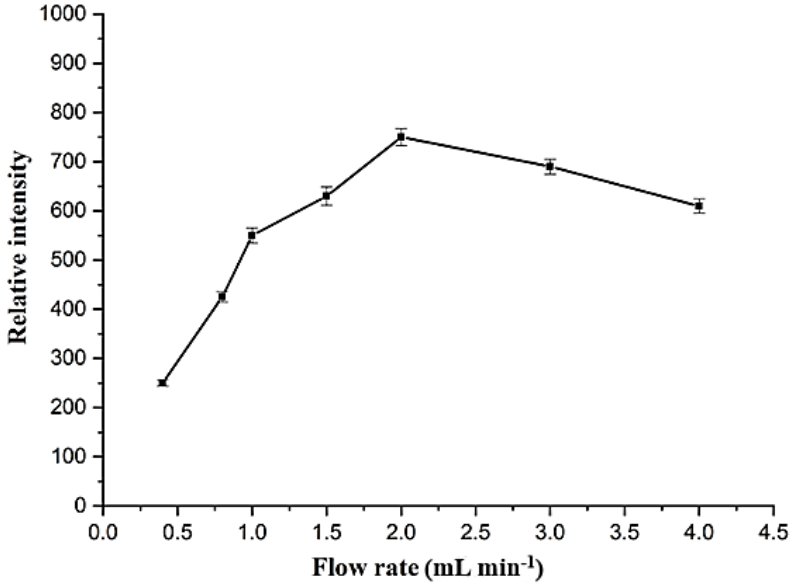

Fig. 6. Effect of using variable flow rates on the CL intensity for the determination of Fe_3O_4 using the proposed CL-FI method under the following experimental conditions: sample loop 100 µL; H_2O_2 concentration 0.006 mmol L^{-1}; luminol concentration 0.5 mmol L^{-1}; Fe_3O_4: 50 µg mL^{-1}

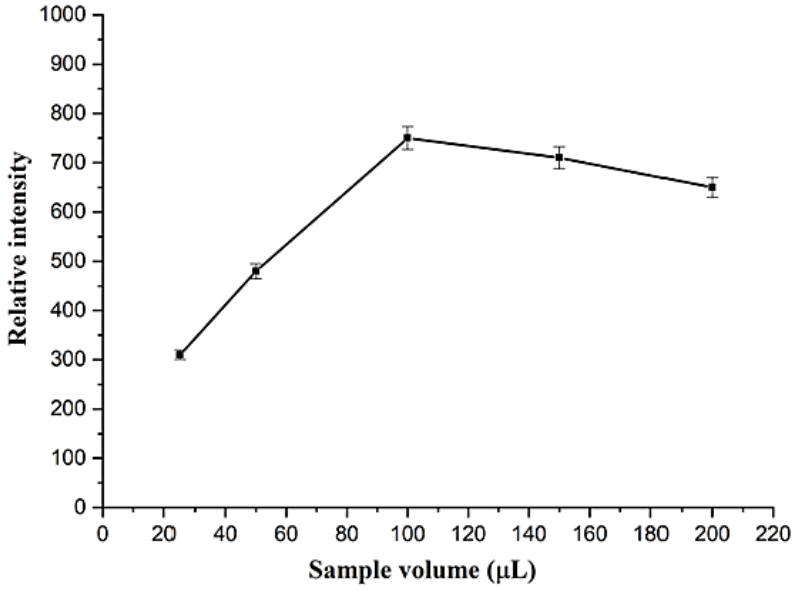

Fig. 7. Effect of using variable sample loops on the CL intensity for the determination of Fe_3O_4 using the proposed CL-FI method under the following experimental conditions: flow rate 2.0 mL min^{-1}; H_2O_2 concentration 0.006 mmol L^{-1}; luminol concentration 0.5 mmol L^{-1}; Fe_3O_4: 50 µg mL^{-1}

Table 2. Summary of ideal operating protocol defined for the CL-FI system

CL-FI parameter	Examined ranges	Selected
[Luminol](mmol L^{-1})	0.05-1.0	0.5
[H_2O_2](mmol L^{-1})	0.002-0.07	0.006
[NaOH] (mmol L^{-1})	0.02-2.0	0.5
Flow rate (mL min^{-1})	0.4- 4.0	2.0
Sample volume (Injected, µL)	25-200	100

3.6. Evaluation of the FI-CL method

A FI-CL method was developed to determine iron oxide using the luminol-NaOH-H_2O_2-Fe_3O_4 system. Method validation studies were performed under optimized operating conditions to evaluate the technique. The linear dynamic range was determined to be 0.5-100 µg mL^{-1} with a limit of detection of 0.47 µg mL^{-1} (calculated as 3σ of the standard error of intercept). The regression equation derived from the linear calibration curve was ΔCL_I = 80.051±3.283+20.787±2.321c, where c is the iron oxide concentration in µg mL^{-1}, and exhibited excellent correlation (R^2 = 0.9970). Intra-assay precision was investigated by analyzing an iron standard of 5.0 µg mL^{-1} eleven times, yielding a relative standard deviation of 2.0%. These quantitative parameters demonstrated the method's suitability for accurate and sensitive measurement of iron oxide levels. Its analytical performance validated the technique and compared favorably to literature methods.

3.7. The effects of potential interferents

The selectivity of the optimized FI-CL method was examined by investigating potential interferences from common excipients. Metal ions present in samples were evaluated for their effects on chemiluminescence intensity. Comparative measurements were made of the CL signal obtained with and without adding individual excipients to a 10 µg mL^{-1} iron oxide standard. The results in Table 3 show that some substances like Cu^{+2}, $Mn^{+2,}$ and Fe^{+2} can interfere by more than 5% relative error under the selected conditions. This demonstrates that pretreatment would be necessary before directly analyzing real black powder samples using this method. X-ray diffraction (XRD) analysis was conducted on the black powder sample to verify the potential presence of interfering metal ions. The XRD results revealed that any amounts of the specified metals were highly minor and below the detection limit of the technique. Therefore, it can be concluded that the examined sample does not contain appreciable quantities

Table 3. Effect of Common Foreign Species on the analysis of 10 µg mL^{-1} Fe_3O_4 by CL method

Interferences species	Tolerance limits
CH_4	100
C_2H_6	100
C_3H_8	100
H_2S	100
Cu^{+2}	5.0
Fe^{+2}	4.0
NO^{3-}	100
Co^{+2}	50
Mg^{+2}	100
CO^{3-}	100
$SO4^{-2}$	100
NH^{4+}	40
Cl^-	50
Cr^{+3}	25
Al^{+3}	20
Zn^{+2}	50
Ni^{+2}	50
Mn^{+2}	8.0
NO^{2-2}	100
Ca^{+2}	75
Na^+	100

of these interfering ions that could impact the analysis. To achieve accurate quantification, interferent matrix components requiring removal or compensation were identified.

3.8. FI-CL analytical method for determination of iron oxide in real black powder sample

Quantitative recovery experiments were performed on real black powder samples according to the established procedure to validate the optimized FI-CL method's applicability. Iron oxide contents determined with the proposed technique were compared to measurements made using an independent X-ray diffraction (XRD) validation method [43]. XRD analysis is the most suitable technique for positively identifying the constituent compounds in the collected black powder samples. XRD employs non-destructive testing utilizing X-rays, crystalline diffraction and Bragg's law. Only a small amount of sample, typically 1 g or less of the black powder, is needed for XRD analysis. The technique generates diffractograms that can be matched to reference patterns to conclusively determine all of the crystalline phase's present in the sample. Through full compositional analysis, XRD allows unambiguous identification of each compound comprising the multi-component black powder. As a well-established method for material characterization, XRD is highly effective for obtaining a complete breakdown of a sample's constituent mineralogical makeup from just a minor quantity of input material. Results presented in Table 4 demonstrate recovery percentages ranging from 92.59% to 107.69% with low precision values (RSD 0.8% - 3.1%). Close agreement was observed between the iron oxide levels in samples derived from FI-CL analysis and those obtained via XRD. This suggests the proposed method offers accuracy comparable to the reference standard when quantifying real-world matrices. The successful recovery study outcomes using authentic test materials establish the validity and reliability of this analytical approach for iron oxide determination in black powder formulations. Quantifying real samples has proven the capabilities of FI-CL to meet validation criteria. Therefore, this flow injection platform can be appropriately applied in laboratory testing.

3.9. Elucidating the underlying chemiluminescence reaction mechanism

This study aims to elucidate the underlying mechanism of the CL reaction involving luminol. Luminol exhibits blue-colored light emission when it undergoes oxidation in a basic environment Figure 8 [44]. However, the detailed steps of the light-generating process have yet to be fully understood. By investigating the roles of key reaction components such as sodium hydroxide, hydrogen peroxide, and iron, we seek insights

Table 4. The analytical results from the analysis of real black powder samples to determine the Fe_3O_4 using the proposed method

Location	Sample weight (g)	Detected (g)	Added (g)	Found (g)	Recovery (%)	RSD[a] (%)	XRD reference [43]
Mosul	0.5	0.11	0.1	0.22	104.76	2.1	0.12
			0.07	0.19	105.50	2.2	
			0.05	0.17	106.25	0.8	
Karbala	0.5	0.17	0.1	0.25	92.59	1.9	0.16
			0.07	0.24	100.00	1.1	
			0.05	0.23	104.54	2.8	
Diwaniya	0.5	0.16	0.1	0.28	107.69	3.1	0.14
			0.07	0.22	95.65	0.9	
			0.05	0.20	95.23	1.4	

[a] Each sample was analyzed in triplicate ($n=3$)

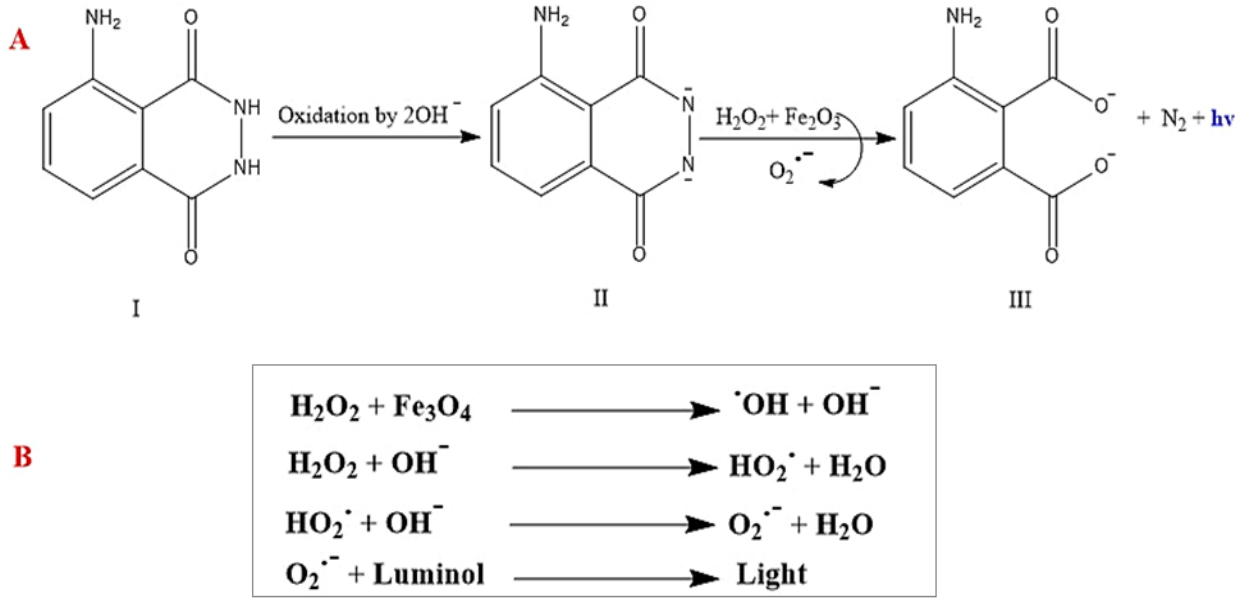

Fig. 8. Mechanism illustration for detection of iron oxide using luminol-H_2O_2-NaOH system. (A): The chemiluminescence process involves the oxidation of luminol ($C_8H_7N_3O_2$, structure I) under moderately basic conditions, which leads to the formation of 3-aminophthalate ion (structure III) as an electronically excited product. Importantly, this 3-aminophthalate intermediate is the light-emitting species responsible for the visible blue emission observed during chemiluminescence. (B): The role of iron oxide in decomposing the H_2O_2.

into how luminol progresses from its initial state to the formation of electronically excited species responsible for photon release. Sodium hydroxide increases the pH of the reaction environment. This promotes the deprotonation of luminol. At high pH, luminol exists predominantly as a dianion due to hydroxide ions' deprotonation of its amino groups [44]. Sodium hydroxide activates luminol by making it more nucleophilic. Fe_3O_4 molecules can catalyze the chemiluminescent reaction due to significantly excess Fe (II) ions on their surfaces [35]. SRXPS analysis revealed that the ratio of Fe (II)/Fe (III) on the Fe_3O_4 surface is around 0.93 [45]. Consequently, in the presence of H_2O_2, these surface Fe (II) ions mediate a heterogeneous Fenton-like reaction, wherein Fe_3O_4 catalyzes the decomposition of H_2O_2 [46]. This decomposition generates reactive superoxide anion radicals (O_2*-), as evidenced by in situ STXM showing the formation of a Fe_2O_3 phase on the surfaces during the reaction. Notably, the superoxide anions rapidly capture luminol, producing an unstable endoperoxide intermediate whose decay results in light emission or chemiluminescence, which can be quantitatively measured for Fe_3O_4 detection. Therefore, Fe_3O_4 effectively catalyzes the chemiluminescent reaction through surface Fe (II)-mediated decomposition of H_2O_2. The unstable organic peroxide then loses a nitrogen molecule (N_2) and undergoes decomposition. During the decomposition process, the electrons of the reaction products change from the triplet excited state to the lower energy ground state. This transition releases energy in the form of a blue-colored photon. The emitted light is the observable chemiluminescence resulting from the overall reaction of luminol dianion with oxygen radicals. Therefore, the combined reaction produces the characteristic blue glow through chemiluminescence. In this mechanism, sodium hydroxide enhances the reaction by increasing pH and activating luminol, allowing the formation of reactive intermediates and excited state emission, leading to light production.

4. Conclusion

In this work, we report the development and validation of a novel FI-CL method for determination of Fe_3O_4 in black powder. The

method exploits the enhancing effect of Fe_3O_4 on the luminol-NaOH-H_2O_2 system. Under optimized conditions, the method demonstrated suitable quantitative performance for Fe_3O_4 detection, with a linear range of 0.5-100 µg mL^{-1}, limit of detection of 0.47 µg mL^{-1}, and intra-assay precision of RSD (2.0%) at 5.0 µg mL^{-1}. Validation studies via real sample analysis of black powder confirmed applicability to complex matrices. A preliminary examination of the underlying chemiluminescence reaction mechanism provided insights into how Fe_3O_4 initiates and amplifies light emission. The automated flow injection format offers rapid analyses, simple operation, and reagent consumption advantages. This new chemiluminescence-based flow injection technique shows promise as a screening tool for Fe_3O_4 quantification, given its demonstrated sensitivity, low cost, and reagent-free nature. Precise Fe_3O_4 analysis thus aids in evaluating pipeline integrity and developing mitigation strategies to prevent fires, explosions, and unplanned outages. It provides critical data for maintaining the safety and reliability of gas transmission operations over the lifetime of pipeline assets.

5. Acknowledgment

The authors thank Prof Dr Issam M. A. Shakir for his support. The authors confirm that there are no relevant financial or non-financial competing interests to report.

6. Reference

[1] P. Q. Gas, Natural gas processing: the crucial link between natural gas production and its transportation to market, Los Alamos, 20 (2006) 1-11.https://www.eia.gov/naturalgas/articles/ngprocessindex.php

[2] M. A. Adewumi, Natural gas transportation issues, J. Pet. Technol., 49 (1997) 139-143. https://doi.org/10.2118/37369-JPT

[3] T. S. Khan, M. S. Al-Shehhi, Review of black powder in gas pipelines–An industrial perspective, J. Nat. Gas Sci. Eng., 25 (2015) 66-76. https://doi.org/10.1016/j.jngse.2015.04.025

[4] G. Guandalini, P. Colbertaldo, S. Campanari, Dynamic modeling of natural gas quality within transport pipelines in presence of hydrogen injections, Appl. Energy, 185 (2017) 1712-1723. https://doi.org/10.1016/j.apenergy.2016.03.006

[5] T. S. Khan, Review of black powder in gas pipelines – An industrial perspective, J. Nat. Gas Sci. Eng., 25 (2015) 423-436. https://doi.org/10.1016/j.jngse.2015.04.025

[6] F. Golbabai, A. Ebrahimi, H. Shirkhanloo, M. R. Baneshi, A. Faghihi, M. J. Kian, Performance comparison survey of multi-walled and single-walled carbon nanotubes for adsorption and desorption and of mercury vapors in air, Iran Occup. Health, 10 (2013) 21-31. https://espace.library.uq.edu.au/view/UQ:9d03f02

[7] F. Golbabaei, A. Ebrahimi, H. Shirkhanloo, A. Koohpaei, A. Faghihi-Zarandi, Single-walled carbon nanotubes (SWCNTs), as a novel sorbent for determination of mercury in air, Global J. Health Sci., 8 (2016) 273-280. https://doi.org/10.5539/gjhs.v8n7p273

[8] H. Shirkhanloo, F. Golbabaei, A. Vahid, A. Faghihi Zarandi, A novel nano-palladium embedded on the mesoporous silica nanoparticles for mercury vapor removal from air by the gas field separation consolidation process, Appl. Nanosci., 12 (2022) 1667-1682. https://doi.org/10.1007/s13204-022-02366-0

[9] H. Shirkhanloo, F. Golbabaei, H. Hassani, F. Eftekhar, M. J. Kian, Occupational exposure to mercury: air exposure assessment and biological monitoring based on dispersive ionic liquid-liquid microextraction, Iran. J. Public Health, 43 (2014) 793-799. http://ijph.tums.ac.ir

[10] A. Sherik, Study examines sources, makeup in dry gas systems, Oil Gas J., 106 (2008) 54-54. https://ogj.com/general-interest/hse/article/17218468/

[11] R. M. Baldwin, Here are procedures

for handling persistent black-powder contamination, Oil Gas J., 96 (1998) 66-75. https://ogj.com/general-interest/hse/article/17218477/

[12] J. He, D. Wang, D. Guo, F. Xie, Y. Qin, Generation causes of black powder in the east line of the gas supply pipeline from the Liaohe oilfield: Analysis and discussion, Eng. Fail. Anal., 139 (2022) 106506. https://doi.org/10.1016/j.engfailanal.2022.106506

[13] J. E. Onwunalu, L. J. Durlofsky, Application of a particle swarm optimization algorithm for determining optimum well location and type, Comput. Geosci., 14 (2010) 183-198. https://doi.org/10.1007/s10596-009-9142-1

[14] A. Bhardwaj, B. Kumar, S. R. Prasad, S. K. Srivastava, Characterization of black powder in gas pipelines, Mater. Perform., 55 (2016) 54-59. https://doi.org/10.1016/B978-0-323-99304-3.00017-0

[15] T. S. Khan, M. Alshehhi, S. Stephen, L. Khezzar, Characterization and preliminary root cause identification of black powder content in a gas transmission network–a case study, J. Nat. Gas Sci. Eng., 27 (2015) 769-775. https://doi.org/10.1016/j.jngse.2015.09.022

[16] R. P. Downham, T. M. Ciuksza, H. J. Desai, V. G. Sears, Black iron (II/III) oxide powder suspension (2009 CAST Formulation) for fingermark visualization, Part 1: Formulation component and shelf-life studies, J. Forensic Identif., 67 (2017) 145-167. https://www.proquest.com/docview/1871397275

[17] W. Taha, M. Abou-Khousa, A. Haryono, M. AlShehhi, K. Al-Wahedi, A. Al-Durra, I. AlNabulsieh, M. Daoud, F. Geuzebroek, M. Faraj, Field demonstration of a microwave black powder detection device in gas transmission pipelines, J. Nat. Gas Sci. Eng., 73 (2020) 103058. https://doi.org/10.1016/j.jngse.2019.103058

[18] R. Turcotte, R. C. Fouchard, A. M. Turcotte, D. E. G. Jones, Thermal analysis of black powder, J. Therm. Anal. Calorim., 73 (2003) 105-118. https://doi.org/10.1023/A:1025181424038

[19] C. L. Crawford, H. Boudries, R. J. Reda, K. M. Roscioli, K. A. Kaplan, W. F. Siems, H. H. Hill Jr, Analysis of black powder by ion mobility−time-of-flight mass spectrometry, Anal. Chem., 82 (2010) 387-393. https://doi.org/10.1021/ac902168a

[20] J. Yamada, H. Kaneta, K. Nakayama, Black powder formation in natural gas pipeline networks: associated issues and root cause analysis, Challenges and Recent Advances in Sustainable Oil and Gas Recovery and Transportation, Chapter 15 (2023) 329-346. https://doi.org/10.1016/B978-0-323-99304-3.00017-0.

[21] T. P. Forbes, J. R. Verkouteren, Forensic analysis and differentiation of black powder and black powder substitute chemical signatures by infrared thermal desorption–DART-MS, Anal. Chem., 91 (2018) 1089-1097. https://doi.org/10.1021/acs.analchem.8b04624

[22] M. Arjomandi, H. Shirkhanloo, A review: analytical methods for heavy metals determination in environment and human samples, Anal. Methods Environ. Chem. J., 2 (2019) 97-126. https://doi.org/10.24200/amecj.v2.i03.73

[23] A. F. Zarandi, H. Shirkhanloo, P. Paydar, A novel method based on functionalized bimodal mesoporous silica nanoparticles for efficient removal of lead aerosols pollution from air by solid-liquid gas-phase extraction, J. Environ. Health Sci. Eng., 18 (2020) 177–188. https://doi.org/10.1007/s40201-020-00450-7

[24] M. K. Hammood, J. N. Jeber, M. A. Khalaf, Rapid colorimetric sensing of chlorpromazine HCl antipsychotic through in situ growth of gold nanoparticles, RSC Adv., 14 (2024) 2327-2339. https://doi.org/10.1039/D3RA05516G

[25] A. Al-Ani, J.N. Jeber, A. Elewi, Development of a nanostructured double-layer coated tablet based on polyethylene glycol/gelatin as a

platform for hydrophobic molecules delivery, Egypt. J. Chem., 64 (2021) 1759-1767. https://doi.org/10.21608/ejchem.2021.52019.3066

[26] N. S. Turkey, J. N. Jeber, Turbidimetric determination of mebeverine hydrochloride in pharmaceutical formulations using two consecutive detection zones under continuous flow conditions, Chem. Chem. Technol., 16 (2022) 600-613. https://doi.org/10.23939/chcht16.04.600

[27] N. S. Turkey, J. N. Jeber, Light scattering detector based on light-emitting diodes-solar cells for a flow analysis of Warfarin in pure form and pharmaceutical formulations, J. Phys.: Conf. Ser.,2063 (2021) 012006. https://doi.org/10.1088/1742-6596/2063/1/012006

[28] N. Jeber Jalal, F. Hassan Raed, K. Hammood Mohammad, Solid phase extraction of theophylline in aqueous solutions by modified magnetic iron oxide nanoparticles as an extractor material and spectrophotometry technique for the determination, Res. J. Chem. Environ., 23 (2019) 94-100. https://www.worldresearchersassociations.com/ChemSpecialMay2019/12.pdf

[29] B. M. Trzcińska, Classification of black powder toners on the basis of integrated analytical information provided by Fourier transform infrared spectrometry and X-ray fluorescence spectrometry, J. Forensic Sci., 51 (2006) 919-924. https://doi.org/10.1111/j.1556-4029.2006.00167.x

[30] M. Iranifam, Revisiting flow-chemiluminescence techniques: pharmaceutical analysis, Lumin., 28 (2013) 798-820. https://doi.org/10.1002/bio.2441

[31] N. S. Turkey, J. N. Jeber, A flow analysis system integrating an optoelectronic detector for the quantitative determination of active ingredients in pharmaceutical formulations, Microchem. J., 160 (2021) 105710. https://doi.org/10.1016/j.microc.2020.105710

[32] J. N. Jeber, N. S. Turkey, An optoelectronic flow-through detectors for active ingredients determination in the pharmaceutical formulations, J. Pharm. Biomed. Anal., 201 (2021) 114128. https://doi.org/10.1016/j.jpba.2021.114128

[33] N. S. Turkey, J. N. Jeber, Flow Injection analysis with turbidity detection for the quantitative determination of mebeverine hydrochloride in pharmaceutical formulations, Baghdad Sci. J., 19 (2022) 141-154. https://doi.org/10.21123/bsj.2022.19.1.0141

[34] J. A. Ocaña-González, M. Ramos-Payán, R. Fernández-Torres, M. V. Navarro, M. Á. Bello-López, Application of chemiluminescence in the analysis of wastewaters–a review, Talanta, 122 (2014) 214-222. https://doi.org/10.1016/j.talanta.2014.01.028

[35] H. Wang, M. Li,B. Wang, M. Wang, I. Kurash, X. Zhang, W. Feng, Magnetic Fe_3O_4 nanoparticle catalyzed chemiluminescence for detection of nitric oxide in living cells, Anal. Bioanal. Chem., 408 (2016) 5479-5488. https://doi.org/10.1007/s00216-016-9646-1

[36] M. J. Chaichi, M. Ehsani, A novel glucose sensor based on immobilization of glucose oxidase on the chitosan-coated Fe_3O_4 nanoparticles and the luminol–H_2O_2–gold nanoparticle chemiluminescence detection system, Sens. Actuators. B Chem., 223 (2016) 713-722. https://doi.org/10.1016/j.snb.2015.09.125

[37] N. Kaewkhomdee, C. Kalambaheti, S. Predapitakkun, A. Siripinyanond, J. Shiowatana, Iron fractionation for corrosion products from natural gas pipelines by continuous-flow sequential extraction, Anal. Bioanal. Chem., 386 (2006) 363-369. https://doi.org/10.1007/s00216-006-0633-9

[38] T. R. Lenhart, K. E. Duncan, I. B. Beech, J. A. Sunner, W. Smith, V. Bonifay, B. Biri, J. M. Suflita, Identification and characterization of microbial biofilm communities associated with corroded oil pipeline surfaces, Biofouling, 30 (2014) 823-835. https://doi.org/10.1080/08927014.2014.931379

[39] R. N. Montagnolli, P. R. Lopes, E. D. Bidoia,

Screening the toxicity and biodegradability of petroleum hydrocarbons by a rapid colorimetric method, Arch. Environ. Contam. Toxicol., 68 (2015) 342-353. https://doi.org/10.1007/s00244-014-0112-9

[40] A. U. Ammar, M. Shahid, M. K. Ahmed, M. Khan, A. Khalid, Z. A. Khan, Electrochemical study of polymer and ceramic-based nanocomposite coatings for corrosion protection of cast iron pipeline, Materials, 11 (2018) 332. https://doi.org/10.3390/ma11030332

[41] L. Chen, D. Xiong, Magnetic techniques for mineral processing, Progress in Filtration and Separation, (2015) 287-324. https://doi.org/10.1016/B978-0-12-384746-1.00007-0

[42] J. R. Dean, Extraction techniques in analytical sciences, John Wiley & Sons, pp. 1-336, 2010. https://www.wiley.com

[43] T. S. Khan, Review of black powder in gas pipelines – An industrial perspective, J. Nat. Gas Sci. Eng., 25 (2015) 66-76. https://doi.org/10.1016/j.jngse.2015.04.025

[44] A. Karabchevsky, A. Mosayyebi, A. V. Kavokin, Tuning the chemiluminescence of a luminol flow using plasmonic nanoparticles, Light sci. Appl., 5 (2016) e16164. https://doi.org/10.1038/lsa.2016.164

[45] S. Yan, S. Ge, W. Qiao, Y. Zuo, Synthesis of ferromagnetic semiconductor 0.67 $FeTiO_3$–0.33 Fe_2O_3 powder by chemical co-precipitation, J. Magn. Magn. Mater., 322 (2010) 824-826. https://doi.org/10.1016/j.jmmm.2009.11.011

[46] X. Xue, K. Hanna, N. Deng, Fenton-like oxidation of Rhodamine B in the presence of two types of iron (II, III) oxide, J. Hazard. Mater., 166 (2009) 407-414. https://doi.org/10.1016/j.jhazmat.2008.11.089